nature geoscience
SUPPLEMENTARY INFORMATION
DOI: 10.1038/NGEO1627

Supplementary Information to "Wind-driven trends in Antarctic sea-ice motion" by

Paul R. Holland and Ron Kwok

Supplementary Methods

Combining ice motion and concentration data allows us to quantify the different processes contributing to the ice concentration budget. The evolution of ice concentration, A, is governed by

$$\frac{\partial A}{\partial t} + \nabla.(\boldsymbol{u}A) = f - r,$$

where $\boldsymbol{u}$ is ice motion, f is the ice concentration change from freezing or melting, and r is the concentration change from mass-conserving mechanical ice redistribution processes, such as ridging, that convert ice area to ice thickness. The results show that redistribution is generally small compared to freezing and melting (see below) so it is neglected here.

Rearranging and integrating over a particular time period, we obtain

$$A(t_2) - A(t_1) = \int_{t_1}^{t_2} f\, dt - \int_{t_1}^{t_2} \boldsymbol{u}.\nabla A\, dt - \int_{t_1}^{t_2} A\nabla.\boldsymbol{u}\, dt,$$

so the ice concentration difference between the end and start of any period is caused by the integrated contributions of freezing, advection, and divergence over that period. In this study the difference term on the left-hand side is calculated between 14-day means of ice concentration data centred upon the end and start of each period. Next, advection and divergence terms are calculated by integrating the relevant daily ice concentration and motion data over the period. Finally, the integrated freezing is determined from the residual of these other terms. We can only calculate these terms for the internal ice pack because the tracking procedure typically fails to capture motion near the ice edge. The formal error in these terms propagates from the quantified error in ice concentration and motion, and in theory is

DOI: 10.1038/NGEO1627

possible to calculate explicitly, but the assumptions required to calculate these errors (specifically the neglect of covariance) are so restrictive as to nullify the utility of the results.

To obtain an overview of the processes contributing to the mean Antarctic ice concentration balance, each of these four terms is calculated for each year and then averaged over our 19-year record

$$\overline{\Delta A} = \overline{\int f} - \overline{\int \boldsymbol{u}.\nabla A} - \overline{\int A\nabla.\boldsymbol{u}},$$

as discussed in the main text. Mean values of the four terms are shown for the whole year (April-October) in Supplementary Figure 1 and for autumn only (April-June) in Supplementary Figure 2. This approach shares some features with a previous method[20]. Passive microwave sea ice data have poorly-quantified seasonal biases (e.g. overestimating ice concentration in summer) that limit the quantitative accuracy of these results[28], but their qualitative overview is extremely infomative.

The 'freezing' term (e.g. Supplementary Figure 1d) is actually the calculation residual and also contains the effects of mechanical redistribution, but it is obvious from the results that it is dominated by thermodynamic processes. The term is generally positive in our non-summer data (an ice concentration source), which clearly represents freezing because it would otherwise require unobserved mechanical processes that convert thick to thin ice. Its negative regions (ice concentration sinks) primarily occur around the ice edge, where ice concentrations are low (< 0.5). When concentrations are low, ice convergence causes concentration to increase, as observed here (Supplementary Figure 1c), rather than decrease through ridging. Therefore we interpret the negative residual around the ice edge as melting, confirming that the residual is mainly thermodynamic. Mechanical processes contribute

significantly to the residual only in the small ice concentration sinks in the western Weddell and Ross seas, where there is strong ice convergence and full ice cover.

With our new 19-year record of ice motion, we can also use this decomposition method to investigate the contribution of dynamic and thermodynamic processes to the observed ice concentration trends. The value of each of the four terms is calculated for each year in our timeseries, and we then calculate the linear trends of these annual values over the 19-year time period τ

$$\frac{\partial\, \Delta A}{\partial \tau} = \frac{\partial \int f}{\partial \tau} - \frac{\partial \int \boldsymbol{u}.\nabla A}{\partial \tau} - \frac{\partial \int A \nabla.\boldsymbol{u}}{\partial \tau}.$$

Trends in autumn (April-June) data are plotted in Supplementary Figure 3 and discussed in the main text. We can then examine the proportional contribution of dynamic processes to the ice concentration trends by considering the ratio between trends in flux divergence (the sum of advection and divergence) and trends in ice concentration difference

$$D = -\frac{\partial \int \nabla.(\boldsymbol{u}A)}{\partial \tau} \Big/ \frac{\partial\, \Delta A}{\partial \tau}.$$

Supplementary Figure 4 shows these two fields and their ratio for our autumn data. Spatial offsets between the two fields lead to small-scale noise in their ratio. Extensive smoothing of the ratio reveals the spatial distribution of the importance of dynamic trends, as discussed in the main text.

DOI: 10.1038/NGEO1627

Supplementary Figures

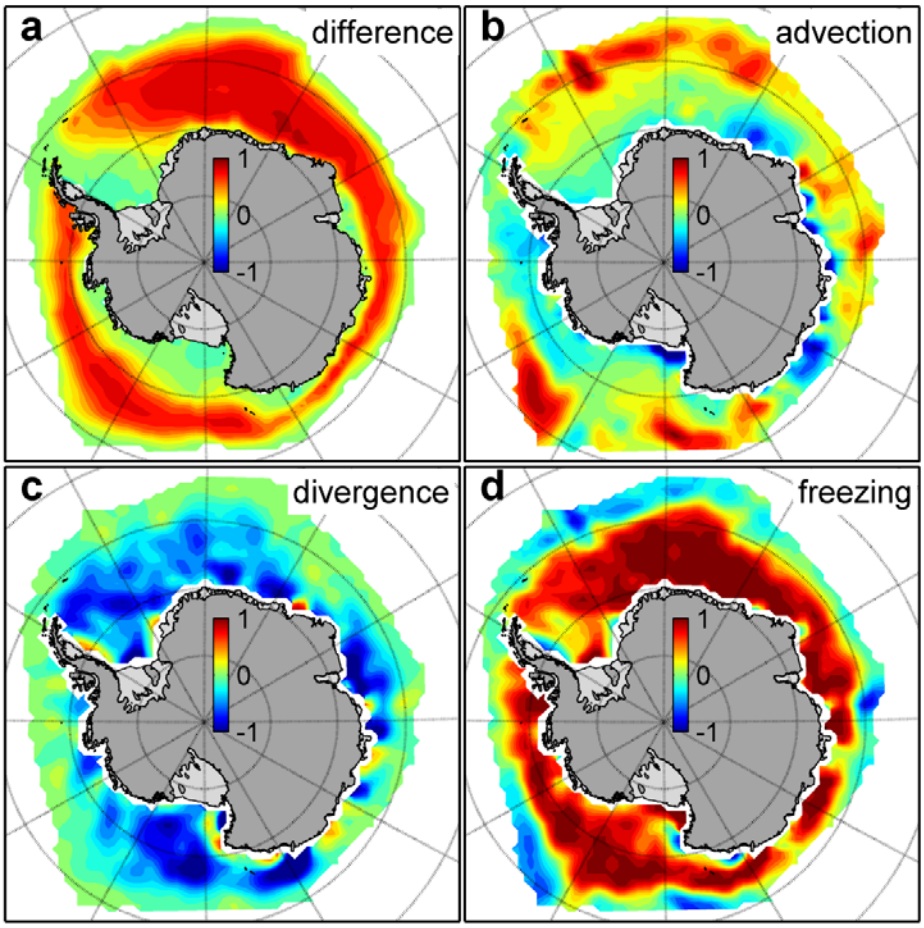

Supplementary Figure 1 | April-October 1992-2010 mean of each component in the ice concentration budget, showing divergence-maintained freezing close to Antarctica and advection-led melting around the ice margins. a) mean observed April-October ice concentration difference, $\overline{\Delta A}$; b) mean concentration difference from observed ice advection, $-\overline{\int \boldsymbol{u}.\nabla A}$; c) mean concentration difference from observed ice divergence, $-\overline{\int A\nabla.\boldsymbol{u}}$; d) mean concentration difference from residual freezing, $\overline{\int f}$. The ice concentration difference in panel a is comprised of the processes in panels b-d. Panels b-d have been smoothed with a 3-point mean to reduce grid-scale noise in the derivatives.

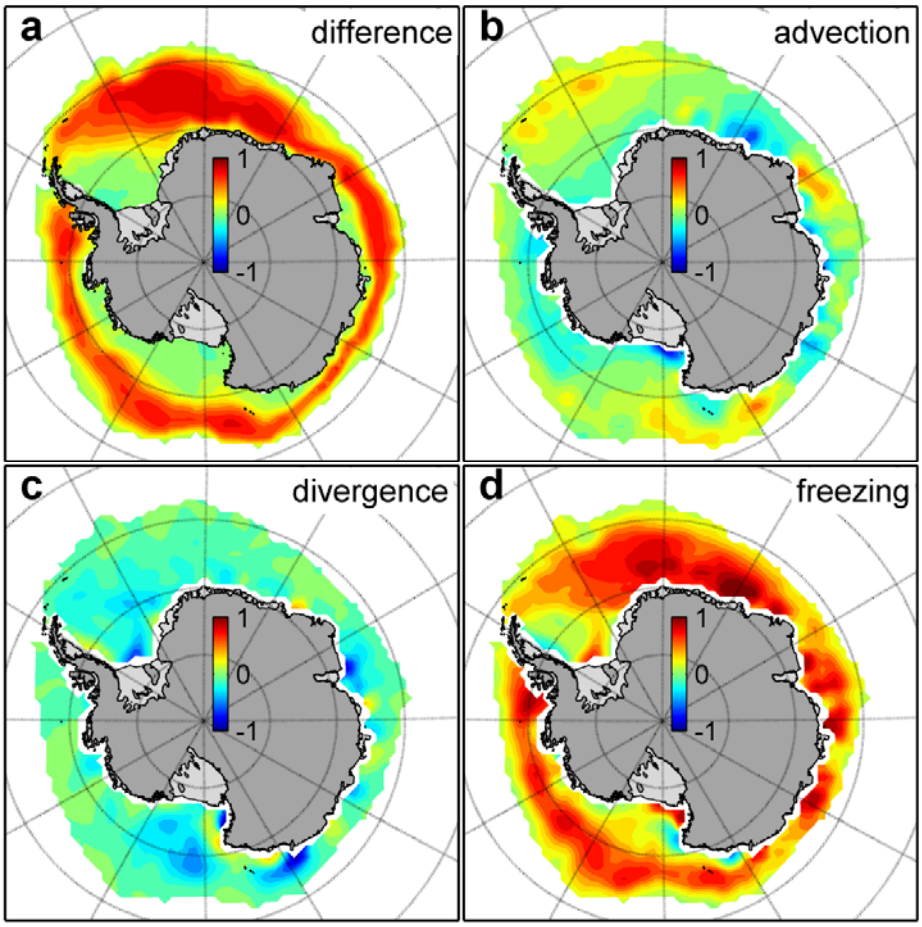

Supplementary Figure 2 | Autumn (April-June) 1992-2010 mean of each component in the ice concentration budget, showing that ice growth is dominated by thermodynamics during this period. Panels calculated as described in Supplementary Figure 1.

DOI: 10.1038/NGEO1627

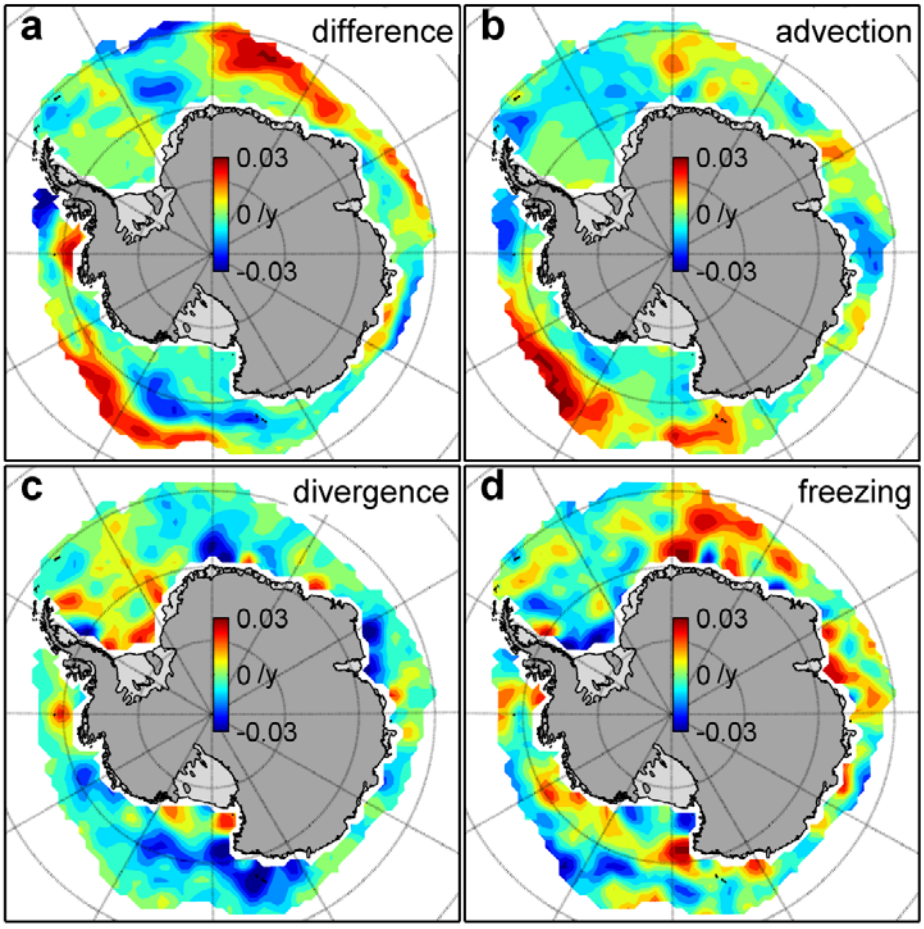

Supplementary Figure 3 | Autumn (April-June) 1992-2010 trends in all components of the ice concentration budget, quantifying the contribution of trends in dynamic and thermodynamic processes to the overall ice concentration trends. a) trend in observed April-June ice concentration difference, $\partial \Delta A/\partial \tau$; b) trend in concentration difference from observed advection, $-\partial \int \boldsymbol{u}.\nabla A/\partial \tau$; c) trend in concentration difference from observed divergence, $-\partial \int A\nabla.\boldsymbol{u}/\partial \tau$; d) trend in concentration difference from residual freezing, $\partial \int f/\partial \tau$; The trend in ice concentration difference shown in panel a is comprised of the trends in the processes shown in panels b-d. Panels b-d have been smoothed with a 3-point mean to reduce grid-scale noise in the derivatives.

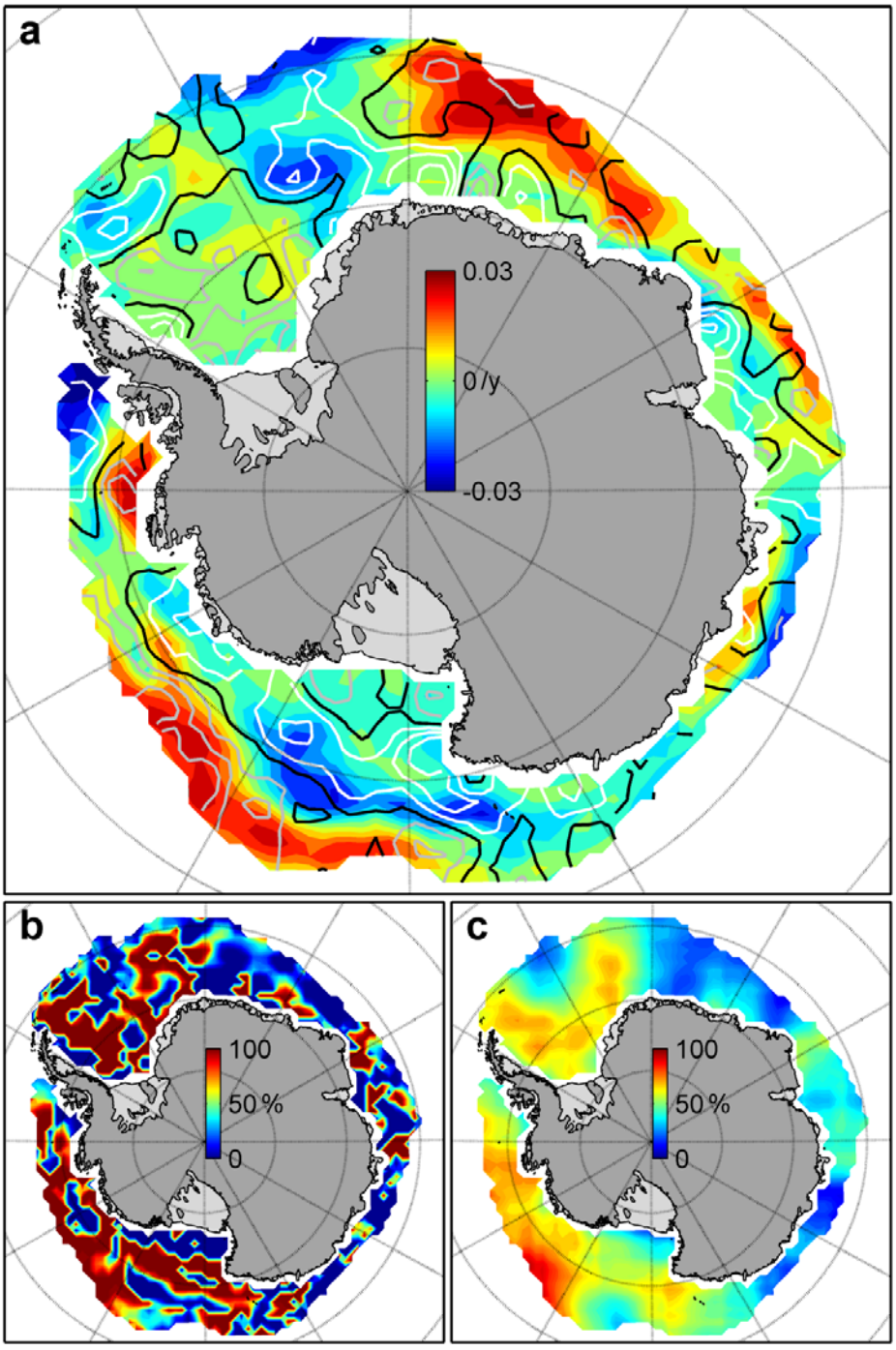

Supplementary Figure 4 | The relation between trends in autumn concentration difference from flux divergence (the sum of advection and divergence) and total trends in autumn ice concentration difference. Extensive smoothing of their ratio reveals a general dominance of dynamic trends in the Pacific sector and Weddell Sea and thermodynamic trends elsewhere. a) trend in ice concentration difference, $\partial \Delta A / \partial \tau$ (underlay), and trend in ice concentration

DOI: 10.1038/NGEO1627

difference from flux divergence, $-\partial \int \nabla.(\boldsymbol{u}A)/\partial\tau$ (overlay; black contour is zero trend, white contours are negative trends, grey contours are positive trends, contour increment 0.01/y); b) unsmoothed fraction of ice difference trend that is explained by the trend in ice difference from flux divergence; c) as panel b but smoothed with a 7-point mean filter.